ELSEVIER

Biophysical Chemistry 69 (1997) 1–8

Biophysical Chemistry

Molecular dynamics simulation of a dye molecule in the interior of a bilayer: 1,6-diphenyl-1,3,5-hexatriene in dipalmitoylphosphatidylcholine

J.J. López Cascales, M.L. Huertas, J. García de la Torre *

Departamento de Química Física, Universidad de Murcia, Campus de Espinardo 30071, Murcia, Spain

Received 8 October 1996; accepted 22 November 1996

Abstract

A Molecular dynamics simulation was carried out for a dipalmitoylphosphatidylcholine (DPPC) membrane in its liquid crystalline state containing different concentrations of the dye molecule 1,6-diphenyl-1,3,5-hexatriene (DPH). From a numerical analysis of the trajectories, we obtained information concerning structural changes of the membrane due to the presence of the probe and some hydrodynamic information concerning the probe itself. The hydrodynamic properties regarding dye molecules that have been reported in this article are: rotational and translational diffusion coefficient and relaxation times. From this analysis, we estimated a range of values of 0.6–0.9 cP for the micro-viscosity in the midmembrane. These simulations also afforded us some information regarding structural changes in the membrane as a consequence of the presence of the fluorescent dyes at different concentrations. Thus, the disorder inside the membrane, the surface area per lipid and thickness of the membrane were also investigated. © 1997 Elsevier Science B.V.

Keywords: MD simulation; DPPC membrane; DPH dye; Structure; Dynamics

1. Introduction

The introduction of fluorescent probes into a membrane is a well known experimental technique for studying dynamic and stationary properties of supra-molecular assemblies such as micelles, lipid bilayers, liquid crystals and cell membranes [1–5].

An experimental technique associated to these molecular probes is the fluorescent anisotropy decay [1,2,6]. When a probe embedded in a membrane is irradiated by an intense polarized light, the emission of fluorescence should be (in principle) strongly polarized too, when the motion of the probe is constrained in some way [7]. From the profiles of the anisotropy decay curves, one can obtain dynamic and stationary properties of the probe, which are somehow associated with the order degree of the environment which is surrounding the probe [8].

Traditionally, the interpretation of a depolarization decay experiment was made in terms of simple hydrodynamics models such as spheres, cylinders or ellipsoids. These simple models only afforded approximations to the real diffusion of probe molecules in such environments. On the other hand, the effect of the presence of probes on the micro-environment in which they resided have not been evaluated properly.

* Corresponding author. E-mail: jgt@fcu.um.es

PII S0301-4622(96)02267-3

1,6-diphenyl-1,3,5-hexatriene (DPH) is one of the most employed molecular probes for these purposes. Due to its complete aromaticity, it behaves as a good chromophore. Furthermore, the absence of any polar groups on this molecule will tend to placed it in the most hydrophobic region of the lipid layers, affording us a very valuable information associated to this region, such as its micro-viscosity.

In this work, we carried out two MD simulations with full atomic detail: first, one probe of DPH in a DPPC (dipalmitoylphosphatidylcholine) membrane in its liquid crystalline state, and second, the number of probes was in the simulation box increased to 3, in condition analogous to the previous case. The membrane was modeled by 72 DPPC distributed in two layers of 36 DPPC each, and 1071 water molecules. From these simulations, we could characterize some dynamics properties related to DPH molecules such as its rotational and translational diffusion coefficients and relaxation time. Indirectly, from the last properties the micro-viscosity inside DPPC bilayers was evaluated. Also a comparison with previous reported simulations of a DPPC membrane in absence of DPH, allowed us to evaluate the effect of the dyes molecules on the lipid structure.

2. Method and models

2.1. Starting up the system

The model of membrane was generated as follows: Two layers of 36 DPPC each were built by copying and rotating a single lipid molecule. A single molecule of DPPC was built by means of the commercial package HyperChem [9]. On both lipid layers, two layers of water molecules of 1.5 nm thick each were placed. The heads of the lipids faced toward the water layers. We used the SPC (single point charge) as the water model [10]. In this way, a three-dimensional periodic box was generated: two layers of lipid were covered by two layers of water molecules. The DPH probes were manually introduced in the hydrocarbon region of the membrane. A DPH molecule was also generated by the commercial package HyperChem [9]. The structure and atom numbering of DPH is shown in Fig. 1. The system was finally composed of: 72 DPPC, 1 or 3 DPH and

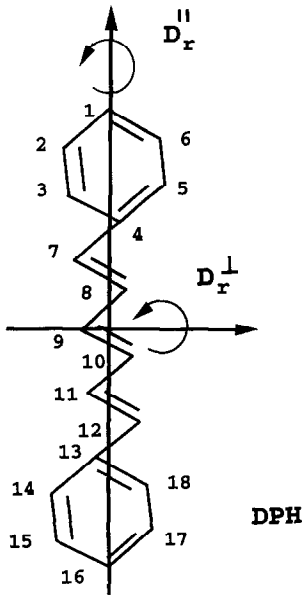

Fig. 1. Atomic numeration and rotation axes of a DPH molecule.

1071 water molecules, which amounts 6851 or 6867 atoms, respectively. The rate probe/lipid is higher than obtained experimentally (1:72 or 1:24 in our simulations against 1:100 in experiments) [3].

Fig. 2 displays a snapshot of the system with one probe.

2.2. MD parameters and simulation

The systems were submitted to a steepest descent energy minimization procedure, followed of 350 and

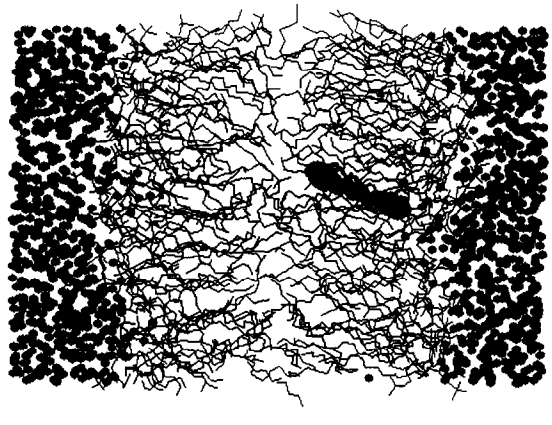

Fig. 2. Snapshot of a DPPC membrane and one DPH molecule.

450 ps of simulations for the systems containing 1 and 3 DPH molecules, respectively. The first 100 and 200 ps, respectively, were discarded due to the fact that the system was not equilibrated. The time step employed along the simulation was 0.002 ps and the neighbouring list was updated every 10 time steeps. The simulations took on the average 20 min ps $^{-1}$ on one R8000 processor of a Silicon Graphics Power Challenge. All calculations shown in this work represents roughly 300 h CPU computer time.

GROMOS [11,12] was the force field employed in our simulations. It was modified as described in previous articles [13–16] where a long cylindrical cut-off was introduced instead of a spherical one and a Ryckaert–Belleman potential [17,18] was used for the 1–4 interactions along the hydrocarbon chains.

The charge distribution on each atom of the lipid molecules and Lennard–Jones parameters were taken from previous simulations [13]. No charges were considered on all DPH atoms.

The system was submitted to a soft coupling bath of pressure and temperature [19]. The simulation was performed at 350 K (well above the transition temperature of 314 K for pure DPPC in aqueous solution [20]) with coupling (dumping) constant of 0.1 ps and pressure of 1 atm with coupling constant of 0.5 ps.

3. Results and discussion

3.1. Dye hydrodynamics

We first describe the rotational dynamics of the probe. Fig. 3 shows the Brownian trajectory of the angle θ subtended by the end-to-end axis of the molecule and the normal to the membrane. The end-to-end vector is defined from atom 1 to 16 of DPH following the atomic dye numeration of Fig. 1. We note how $\cos\theta$ fluctuates between 1 (perpendicular to the membrane) and about 0.2 (roughly parallel). However, $\cos\theta$ does not become negative during the simulation time; in other words, no 'flip–flop' is observed; the probe is unable to reverse its direction in 250 ps.

The tumbling end-to-end rotational dynamics is characterized by means of the temporal evolution of the second Legendre polynomial $\langle P_2(t)\rangle_e$ defined by:

$$\langle P_2(t)\rangle \equiv \langle \vec{u}(t)\vec{u}(0)\rangle \qquad (1)$$

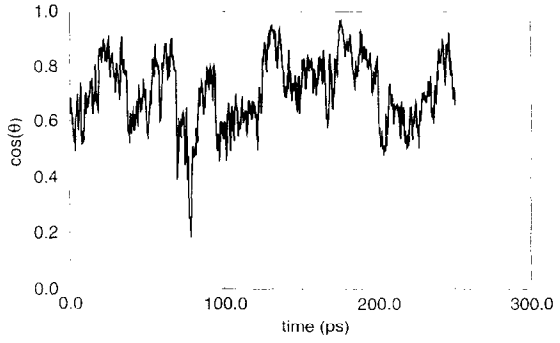

Fig. 3. Temporal evolution of the cosine of the angle formed by the end-to-end DPH vector and normal axis to the membrane plane.

where $\vec{u}(0)$ is the end-to-end unitary vector of the probe at some (initial) time, and $\vec{u}(t)$ has the same meaning than $\vec{u}(0)$ after a time t has elapsed. In this regard, $\langle P_2(t)\rangle_e$ is a function related to the decay fluorescence anisotropy, $r(t)$, in experiments with fluorescent probes [8]. Actually, when either the absorption or the emission dipole are along the molecular axis, $\langle P_2(t)\rangle_e$ is the normalized decay, i.e., $\langle P_2(t)\rangle_e = r(t)/r(0)$. Fig. 4 displays the simulation results for $\langle P_2(t)\rangle_e$ over 50 ps. The length of the trajectory does not allow calculate $\langle P_2(t)\rangle_e$ at longer times.

In order to include in our study the rotational diffusion around the molecular axis, we have moni-

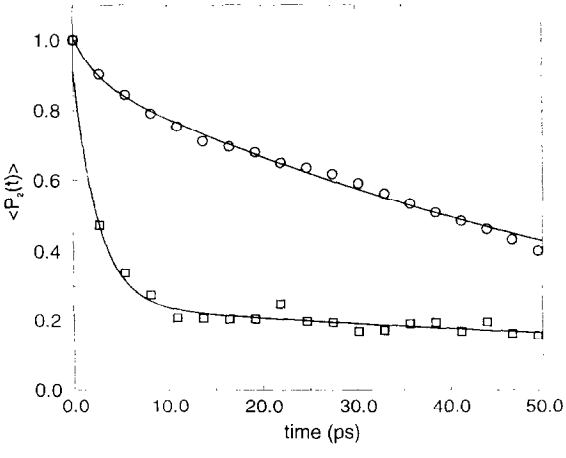

Fig. 4. Long time evolution of $\langle P_2\rangle$ of the end-to-end DPH vector (○) and the perpendicular vector to the phenyl plane (□).

tored the motion of a vector perpendicular to the any of the two phenyl rings, and we have made a similar correlation analysis to calculate the $\langle P_2(t)\rangle_{ph}$ function corresponding to this vector. In Fig. 4 we display the results.

For the characterization of the kinetics of the $\langle P_2(t)\rangle$ decays it is a common practice to fit them to a sum of exponential terms by a nonlinear least square procedure, i.e.,

$$\langle P_2(t)\rangle = \sum_{i=1}^{n} a_i \exp(-t/\tau_i) \qquad (2)$$

where τ_i are the rotational correlation times. In the most cases, the fit of Eq. (2) is not improved by including terms beyond $n = 2$.

The mean rate of kinetics of $\langle P_2(t)\rangle$ decays can be characterized in terms of a relaxation time τ_{mean} which is obtained from [21],

$$\tau_{mean} = \frac{\sum_{j=1}^{2} a_i \tau_i}{\sum_{j=1}^{2} a_i} \qquad (3)$$

where τ_i possess the meaning of Eq. (2).

From Eq. (3), a value of 0.061 ns was obtained for the mean rotational relaxation time of the end-to-end tumbling, $\tau_{mean,e}$, and 0.0051 ns for the rotation relaxation time of the vector normal to the benzene rings in the molecule ($\tau_{mean,ph}$). From MD simulation of benzene embedded in a DMPC (dimyristoylphosphatidylcholine) membrane at 320 K [22] a reorientational correlation time of 0.025 ns was obtained. This result agrees quite well with ours, on the basis of that the DPH molecule is larger than the benzene molecule and realizing about the different temperatures at which both simulations were performed.

The relaxation rate, and particularly the τ_{mean} relaxation times for both vectors, are complex combinations of the main rotational diffusion coefficients of the molecule, $D_r^{\perp}$ and $D_r^{\parallel}$. However, hydrodynamic theory predicts that the relaxation at very short times depends very easily of the end-to-end coefficient. Actually, from the evolution of $\langle P_2(t)\rangle$ in a very short range of times (in our case from 0 to 5 ps), an initial relaxation time, τ_{ini}, can be evaluated from the following expression [23]:

$$\tau_{ini} = -\left(\mathrm{d}\ln\langle P_2(t)\rangle/\mathrm{d}t\right)^{-1}_{t\to 0} \qquad (4)$$

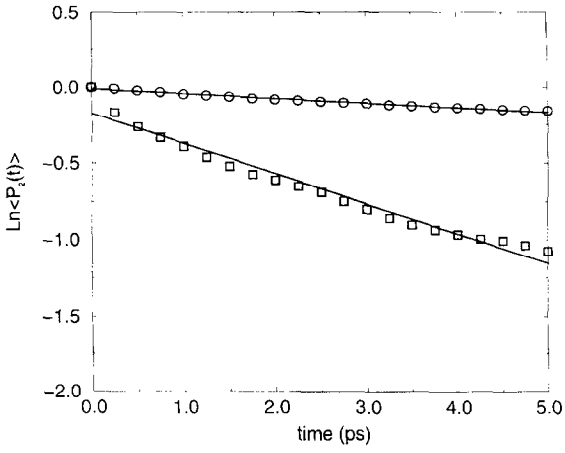

Fig. 5. Short time evolution of ln $\langle P_2\rangle$ for the end-to-end DPH vector (○) and the perpendicular one to the phenyl plane (□).

Values $\tau_{ini,e}$ and $\tau_{ini,ph}$ can be so defined, for the end-to-end vector and the perpendicular vector of the molecule.

Fig. 5 displays the linear regression of $\ln\langle P_2(t)\rangle$ versus time, in a range of 5 ps. According to hydrodynamic theory, the perpendicular rotational diffusion coefficient $D_r^{\perp}$ (see Fig. 1) of the dye molecule is related to the initial relaxation time $\tau_{ini,e}$ [7,23–25] by means of the following equation:

$$\tau_{ini,e} = \frac{1}{6D_r^{\perp}} \qquad (5)$$

From our decay curve, a value $\tau_{ini,e}^{\perp} = 0.03$ ns was obtained, from which we evaluate a rotational diffusion coefficient $D_r^{\perp} = 52 \times 10^8\ s^{-1}$. Unfortunately, there are no experimental data available for a direct comparison. From experimental results of DPH in paraffin oil at lower temperatures [4], we extrapolate at 350 K a value of $47 \times 10^7\ s^{-1}$. These two values are hardly comparable; the difference may be associated to the very short time scale (5 ps) in our analysis of $\tau_{ini,e}$ in which the motion of our molecule is mostly vibrational. We recall that the results from simulations are typically one order of magnitude above the experimental ones.

A similar analysis of $\langle P_2(t)\rangle_{ph}$ at the initial 5 ps has been carried out, which yields $\tau_{ini,ph} = 0.0051$ ns, i.e., about 5 ps. This time is so short that it may correspond essentially to internal vibrations, and it is

clearly risky to relate it to hydrodynamic coefficients.

An effective micro-viscosity associated to the interior of the membrane can roughly be estimated from the Einstein equation, which relates the rotational diffusion coefficient with the micro-viscosity (supposedly a continuum medium) [4],

$$\eta = \frac{k_B T}{6 D_r^{\perp} V} \tag{6}$$

This assumes that the molecule is spherical, and we take for V the van der Waals volume. $k_B T$ is the Boltzman's constant, and $D_r^{\perp}$ is the perpendicular rotational diffusion coefficient. Using a value of 233 Å^3 for V [4] and the value of $D_r^{\perp} = 52 \times 10^8$ s^{-1} from our simulations, we obtained a microviscosity of 0.6 cP inside the membrane. If we had taken an effective volume V_{eff} of 161 Å^3 [4], the resulting micro-viscosity would be 0.9 cP. These value agrees well with the range of 0.84 to 1.4 cP previously reported for a DPPC membrane [26].

Regarding translational diffusion, we splitted up the dye centre-of-mass motion in two directions: on the plane of the membrane and along the perpendicular axis to the membrane, with diffusion coefficients D_t^{lat} and D_t^{transv}, respectively [23]. Fig. 6 shows the trajectory of the centre of mass in the z direction. From this plot, we note that the probe motion is clearly clustered in the hydrophobic region of the membrane, spending only some time in regions near the interface lipid–water.

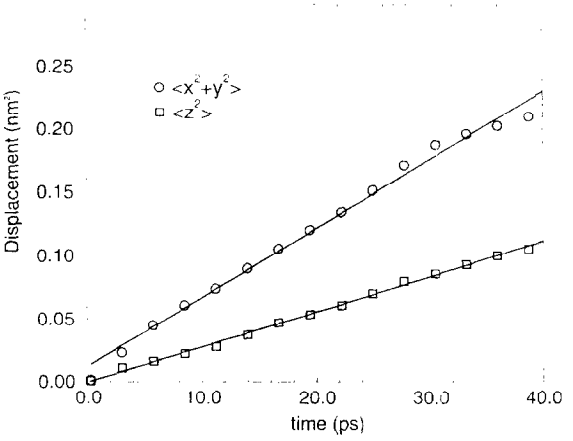

Fig. 7. Parallel and perpendicular displacements of the DPH respect the membrane plane.

From Fig. 6 and similar plots for the x and y coordinates, we learn that the mean displacement of the molecule over 250 ps is of a few Å. Hence, we anticipate that the diffusion coefficients resulting from our analysis are an estimation.

Fig. 7 displays the correlation displacements as a function of the time. From Einstein equation, we can

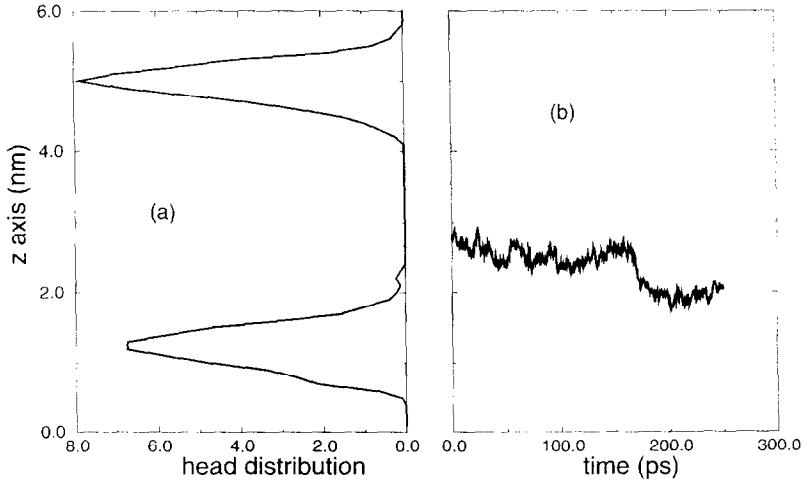

Fig. 6. Motion of the centre-of-mass of a dye molecule embedded in the membrane (b), and profile of the head lipid distribution across the membrane was also plotted (a).

relate the displacements to the translational diffusion coefficient as follows:

$$\langle x^2 + y^2 \rangle = 4D_t^{\text{lat}} t$$
$$\langle z^2 \rangle = 2D_t^{\text{transv}} t \quad (7)$$

where the x and y axes are on the membrane plane and the z axis is perpendicular to the membrane. From the slope of both curves, we estimated $D_t^{\text{lat}} = 1.36 \times 10^{-5}$ cm^2 s^{-1} and $D_t^{\text{transv}} = 1.4 \times 10^{-5}$ cm^2 s^{-1}. Some values for the translational diffusion coefficient [22] of benzene in a DMPC membrane at 320 K have been measured by MD simulation, which ranged from 1.2 to 4.2×10^{-6} cm^2 s^{-1}. The difference may be largely due to the difference in temperature.

3.2. Membrane structure

An important aspect in our study is the effect of the presence of a dye molecule on the membrane structure. In this regard, a property to be investigated is the surface area per lipid. From our simulations in presence of one DPH molecule (DPH:DPPC = 1:72), a surface area of 0.60 nm^2 was measured, very close to the experimental value of 0.59 nm^2 of a DPPC membrane in its liquid crystalline state [20]. When 3 DPH molecules were introduced into the membrane (DPH:DPPC = 3:72), the surface area per lipid was slightly reduced to 0.56 nm^2.

Regarding the membrane thickness (defining this as the distance between the two maxima of the head lipid distributions (Fig. 6)), we obtained a value of 3.7 nm compared to the value of 3.6 nm [27] from a MD simulation of a DPPC membrane in absence of DPH. When 3 DPH were introduced, the membrane thickness was reduced to 3.5 nm.

Bassolino-Klimas et al. [22] carried out a MD simulation of a DMPC membrane in its liquid crystalline state with a variable number of benzene molecules embedded into the membrane. They shown no changes in the membrane thickness and surface area per lipid when benzenes were dissolved till very high concentrations of molecules were added. Analogous behaviour has been obtained by X-ray and neutron diffraction of the effect of general anaesthetics on the structure of lipid bilayers [28]. Analogous results have been provided from deuterium nuclear magnetics resonance (NMR) spectroscopy of local anaesthetics in membranes [29].

Perhaps, the most sensitive property to change along the hydrocarbon chain is the deuterium order parameter, S_{CD}. From simulation, the deuterium order parameter is computed as follows:

$$S_{\text{CD}} = \frac{2S_{xx}}{3} + \frac{S_{yy}}{3} \quad (8)$$

where S_{xx} and S_{yy} are the terms of the order parameter tensor S defined as:

$$S_{\alpha\beta} = \frac{\langle 3\cos\theta_\alpha \cos\theta_\beta - \delta_{\alpha\beta} \rangle}{2},$$
$$\alpha = x, y, z; \beta = x, y, z \quad (9)$$

where θ_i is the angle between the ith molecular axis and the normal to the bilayer and $\delta_{\alpha\beta}$ is the Kronecker delta. The bilayer x and y axes were taken on the membrane plane and z is normal to the membrane plane. A more detailed information can be obtained from previous articles (Refs. [13,15]).

Table 1 shows the order parameters along the hydrocarbon lipid tails obtained from our simulation, compared to experimental and simulation results. We observe how in presence of only one dye, for a dye/lipid ratio of 1:72 the disorder is increased along the lipid tails. This effect is notably augmented

Table 1
Order parameter ($-S_{\text{CD}}$) along the hydrocarbon chains

Carbon number	DPPC[a]	DMPC[b]	DMPC[c]	DPPC[d]	DPPC[e]
3	0.16	0.20	0.18	0.12	0.06
4	0.17	0.21	0.18	0.11	0.05
5	0.15			0.12	0.04
6	0.16	0.21	0.16	0.09	0.03
7				0.08	0.04
8	0.15	0.18	0.14	0.10	0.04
9	0.14			0.09	0.04
10	0.09	0.16	0.11	0.09	0.09
11				0.04	0.01
12	0.10	0.04	0.08	0.06	0.02
13				0.05	0.04
14	0.07			0.04	0.01

[a] Experimental $-S_{\text{CD}}$ of a DPPC membrane at 353 K [31].
[b] Experimental $-S_{\text{CD}}$ of a membrane of dimyristoylphosphatidylcholine (DMPC) at 313 K [29].
[c] Experimental $-S_{\text{CD}}$ of a DMPC membrane + benzyl-alcohol at 313 K [29].
[d] Simulation $-S_{\text{CD}}$ of a DPPC membrane + 1DPH at 350 K, this work.
[e] $-S_{\text{CD}}$ of DPPC + 3DPH at 350 K, this work.

with the number of dyes embedded in the membrane. In this regard, some theories have suggested that anaesthetics elicited their response by disrupting membrane structure reducing in this way the order parameter of the lipid tails [28–30]. From MD simulation, Bassolino-Klimas et al. [22] measured the variation of the order parameter along the hydrocarbon tails of DMPC lipids when benzene molecules were dissolved into the membrane. These results remark the trend of ours, where an increasing of the number of molecules dissolved into the membrane reduced the order parameter along the lipid hydrocarbon tails, becoming this effect more remarkable near the first ethylene atoms of the lipid chain, where less free space is available and the presence of the probe (either DPH or benzenes) is felt more strongly, resulting in the noticeable decrease in ordering of the chains.

4. Conclusion

From MD simulations with full atomic detail of a DPPC membrane in presence of different concentration of dye molecules, we found how the presence of such probes disturb the membrane structure. Thus, the order parameter along the ethylene lipid tails decreases. This effect is more noticeable when the concentration of probes was increased. On the other hand, other properties such as the surface area per lipid and thickness of the tail region did not suffer significant changes when these were compared to DPPC membranes in absence of solutes or probes.

Concerning the probe hydrodynamic properties, the values obtained from our calculations agree quite well with experimental ones. In this regard, rotational and translational diffusion coefficients fall in the range of previous measured values, employing for such calculations simple hydrodynamics models such as spheres or ellipsoids. We were able to estimate the micro-viscosity for the midmembrane, emerging a value very close to previous experimental and simulation ones, where a value around 1 cP was measured.

Acknowledgements

We are very grateful to Prof. H.J.C. Berendsen (University of Groningen, The Netherlands) for his continuing advice and support. The present problem was suggested to us by Prof. A.U. Acuña (Consejo Superior de Investigaciones Cientificas, Madrid, Spain), to whom we are indebted for his interest and essential information. J.J.L.C. thanks the Spanish Government his financial support through a Contrato de Reincorporacion de Doctores. M.H.T. also acknowledges the same source the award of a fellowship of the Plan de Formacion de Profesorado Universitario. This work was supported by grant PB93-1132 (Direccion General de Universidad e Investigacion), and grant CII*-CT94-0124 (Program of International Scientific Cooperation, Commission of the European Communities).

References

[1] P.M. Bayley, R. Dale, Spectroscopy and Dynamics of Molecular Biological Systems, Academic, New York, 1985.
[2] L.M. Loew, Spectroscopy of Membrane Probes, CRC Press, Boca Raton, 1988.
[3] C.R. Mateo, Ph.D. Thesis, Universidad Autonoma de Madrid, Fac. de Ciencias, Departamento de Quimica., 1989.
[4] C.R. Mateo, M.P. Campillo, J.R. Brochon, M.P. Martínez-Ripoll, J. Sanz-Aparicio, A.U. Acuña, J. Phys. Chem. 14 (1993) 3468.
[5] A.U. Acuña, M.P. Lillo, J. González-Rodríguez, C.R. Mateo, K.R. Naqvi, Pure Appl. Chem. 9 (1992) 1211.
[6] T.M. Jovin, M. Bartholdi, W.L.C. Vaz, R.H. Austin, Ann. NY Acd. Sci. 366 (1981) 176.
[7] A. Szabo, J. Chem. Phys. 81 (1984) 150.
[8] Ph. Yeagle (Ed.), The structure of Biological Membranes, CRC Press, New York, 1992.
[9] HyperChem. Package developed by and licensed from HyperCube, Inc., 1992.
[10] H.J.C. Berendsen, J.P.M. Postma, W.F. van Gunsteren, J. Hermans, in: B. Pullman (Ed.), Intermolecular Forces, Reidel, Dordrecht, 1981, p. 331.
[11] W.F. van Gunsteren, H.J.C. Berendsen, GROMOS: GROningen MOlecular Simulation (software package), Biomos, Nijenborgh 4, 9747 AG Groningen, The Netherlands, 1987.
[12] W.F. van Gunsteren, H.J.C. Berendsen, Angew Chem., Int. Ed. Engl. 29 (1990) 992.
[13] S.J. Marrink, H.J.C. Berendsen, J. Phys. Chem. 15 (1994) 4155.
[14] S.J. Marrink, M. Berkowitz, H.J.C. Berendsen, Langmuir 11 (1993) 3122.
[15] J.J. López Cascales, J. García de la Torre, S.J. Marrink, H.J.C. Berendsen, J. Chem. Phys. 7 (1996) 2713.
[16] J.J. López Cascales, H.J.C. Berendsen, J. García de la Torre, J. Phys. Chem 21 (1996) 8621.

[17] J.P. Ryckaert, A. Bellemans, Chem. Phys. Lett. 30 (1975) 123.
[18] J.P. Ryckaert, A. Bellemans, Faraday Discuss. Chem. Soc. 66 (1978) 1978.
[19] H.J.C. Berendsen, J.P.M. Postma, W.F. van Gunsteren, A. DiNola, J.R. Haak, J. Chem. Phys. 8 (1984) 3684.
[20] L.R. De Young, K.A. Dill, Biochemistry 27 (1993) 5281.
[21] R.M. Venable, Y. Zhang, B.J. Hardy, R.W. Pastor, Science 262 (1993) 223.
[22] D. Bassolino-Klimas, H.E. Alper, T.R. Stouch, Biochemistry 32 (1993) 12624.
[23] M.L. Huertas, V. Cruz, J.J. López Cascales, A.U. Acuña, J. García de la Torre, Biophys. J. 71 (1996) 1248.
[24] G. Lipari, A. Szabo, Biophys. J. 30 (1980) 489.
[25] W. van der Meer, H. Pottel, W. Herreman, M. Ameloot, H. Hendricks, H. Schroder, Biophys. J. 46 (1984) 525.
[26] R.W. Pastor, R.M. Venable, M. Karplus, J. Chem. Phys. 89 (1988) 1112.
[27] E. Egberts, S.J. Marrink, H.J.C. Berendsen, Eur. Biophys. J. 22 (1994) 423.
[28] N.P. Franks, W.R. Lieb, J. Mol. Biol. 133 (1979) 469.
[29] G.L. Turner, E. Oldfield, Nature 227 (1977) 669.
[30] R.G. Ashcroft, H.G.L. Coster, J.R. Smith, Nature 269 (1977) 819.
[31] M.F. Brown, J. Phys. Chem. 3 (1982) 1576.